Report

Cell Reports

A Mouse Model of X-linked Intellectual Disability Associated with Impaired Removal of Histone Methylation

Graphical Abstract

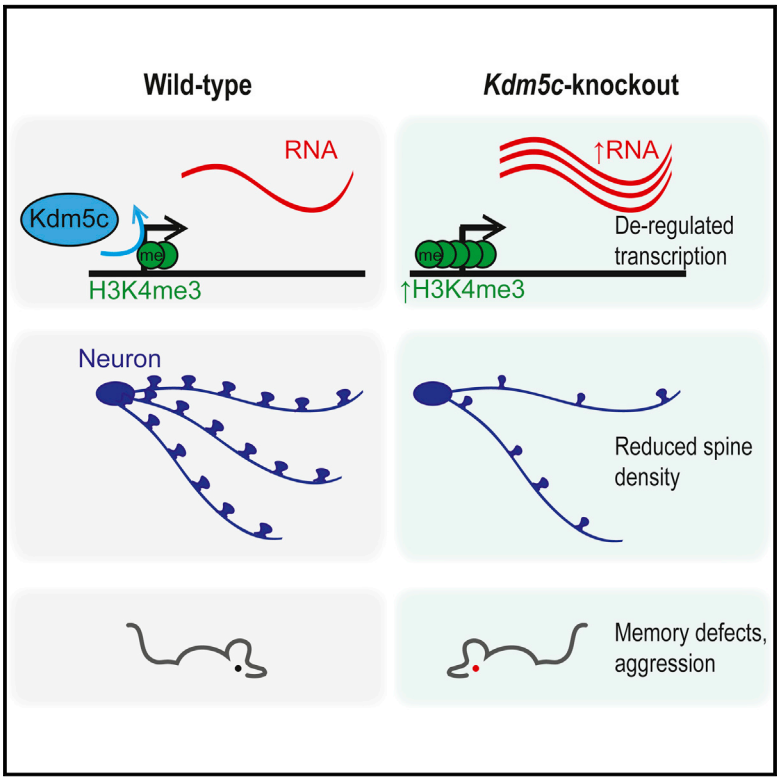

Highlights

- Behavior of *Kdm5c*-knockout mice recapitulates *KDM5C*-linked intellectual disability
- Kdm5c is required for normal dendritic branching and spine morphology in vivo
- Kdm5c acts as a repressor through reducing H3K4me3 levels at CpG promoters

Authors

Shigeki Iwase, Emily Brookes, Saurabh Agarwal, ..., Brian Egan, Jun Xu, Yang Shi

Correspondence

siwase@umich.edu (S.I.), junxu@vetmed.wsu.edu (J.X.), yshi@hms.harvard.edu (Y.S.)

In Brief

In this study, Iwase et al. characterize *Kdm5c*-knockout mice to model an important class of intellectual disability. *Kdm5c*-knockout mice show limited learning, heightened aggression, and dendritic spine defects. Kdm5c is a histone demethylase, and the authors identify altered transcriptional profiles in *Kdm5c*-knockout brains and investigate the molecular changes in neurons.

Accession Numbers

GSE61036

Iwase et al., 2016, Cell Reports *14*, 1000–1009
February 9, 2016
http://dx.doi.org/10.1016/j.celrep.2015.12.091

OPEN ACCESS
CellPress

Cell Reports
Report

A Mouse Model of X-linked Intellectual Disability Associated with Impaired Removal of Histone Methylation

Shigeki Iwase,[1,2,9,*] Emily Brookes,[1,9,10] Saurabh Agarwal,[2,9] Aimee I. Badeaux,[1] Hikaru Ito,[3] Christina N. Vallianatos,[2] Giulio Srubek Tomassy,[4] Tomas Kasza,[2] Grace Lin,[5] Andrew Thompson,[6] Lei Gu,[1] Kenneth Y. Kwan,[5] Chinfei Chen,[6] Maureen A. Sartor,[7] Brian Egan,[8] Jun Xu,[3,*] and Yang Shi[1,*]

[1]Division of Newborn Medicine, Boston Children's Hospital and Department of Cell Biology, Harvard Medical School, 300 Longwood Avenue, Boston, MA 02115, USA
[2]Department of Human Genetics, University of Michigan, 5815 Medical Science II, Ann Arbor, MI 48109, USA
[3]Department of Integrative Physiology and Neuroscience, Washington State University, 1815 Ferdinand's Lane, Pullman, WA 99164, USA
[4]Department of Stem Cell and Regenerative Biology, Harvard University, 7 Divinity Avenue, Cambridge, MA 02138, USA
[5]Molecular & Behavioral Neuroscience Institute and Department of Human Genetics, University of Michigan, Ann Arbor, MI 48109, USA
[6]Department of Neurology, F.M. Kirby Neurobiology Center, Boston Children's Hospital, Harvard Medical School, 300 Longwood Avenue, Boston, MA 02115, USA
[7]Department of Computational Medicine and Bioinformatics, University of Michigan, 100 Washtenaw Avenue, Ann Arbor, MI 48109, USA
[8]Active Motif Inc., Carlsbad, CA 92008, USA
[9]Co-first author
[10]Present address: MRC Laboratory for Molecular Cell Biology, University College London, Gower Street, London WC1E 6BT, UK
*Correspondence: siwase@umich.edu (S.I.), junxu@vetmed.wsu.edu (J.X.), yshi@hms.harvard.edu (Y.S.)
http://dx.doi.org/10.1016/j.celrep.2015.12.091

SUMMARY

Mutations in a number of chromatin modifiers are associated with human neurological disorders. KDM5C, a histone H3 lysine 4 di- and tri-methyl (H3K4me2/3)-specific demethylase, is frequently mutated in X-linked intellectual disability (XLID) patients. Here, we report that disruption of the mouse *Kdm5c* gene recapitulates adaptive and cognitive abnormalities observed in XLID, including impaired social behavior, memory deficits, and aggression. *Kdm5c*-knockout brains exhibit abnormal dendritic arborization, spine anomalies, and altered transcriptomes. In neurons, Kdm5c is recruited to promoters that harbor CpG islands decorated with high levels of H3K4me3, where it fine-tunes H3K4me3 levels. Kdm5c predominantly represses these genes, which include members of key pathways that regulate the development and function of neuronal circuitries. In summary, our mouse behavioral data strongly suggest that *KDM5C* mutations are causal to XLID. Furthermore, our findings suggest that loss of KDM5C function may impact gene expression in multiple regulatory pathways relevant to the clinical phenotypes.

INTRODUCTION

Chromatin is composed of repeating units of nucleosomes, each comprising ~146 base pairs of DNA wrapped around an octamer of histones H2A, H2B, H3, and H4 (Luger et al., 1997). Post-translational modifications of histones affect a variety of chromatin template-based events, including transcription, replication, and DNA repair (Kouzarides, 2007). Chromatin dysregulation has emerged as a major contributor to neurodevelopmental (Iwase and Shi, 2010) and psychiatric (Nestler, 2014) disorders. Intellectual disability (ID) is a prevalent brain disorder, affecting 1%–2% of the total population, and represents a major unmet medical need worldwide. ID is defined as limitations in both adaptive behavior and intellectual functioning (van Bokhoven, 2011). Advances in DNA sequencing technologies have led to the identification of genetic variations associated with ID, including mutations in many chromatin regulators, e.g., genes encoding enzymes that add or remove chemical modifications from DNA or histone, enzymes that affect nucleosome positioning, and reader proteins that recognize specific chromatin modifications (Iwase and Shi, 2010). Despite the identification of genetic variations associated with different forms of ID, the cellular and molecular etiology of ID remains poorly understood.

KDM5C (also known as *SMCX* and *JARID1C*) is an X-linked gene whose protein product belongs to a subfamily of JmjC domain histone demethylases that mediate demethylation of histone H3K4me2/3 (Iwase et al., 2007; Tahiliani et al., 2007). Human genetic studies identified an association between *KDM5C* mutations and X-linked ID (XLID), estimated to account for 0.7%–2.8% of all XLID cases (Gonçalves et al., 2014; Ropers and Hamel, 2005). Patient mutations in *KDM5C* include nonsense and missense mutations; all patient missense mutations tested compromise KDM5C's enzymatic activity, suggesting a loss-of-function disease mechanism (Brookes et al., 2015; Iwase et al., 2007; Tahiliani et al., 2007). In addition to ID (ranging from

mild to severe), many patients with *KDM5C* mutations exhibit physical and behavioral abnormalities, including short stature, epilepsy, aggressive or violent behavior, and constant smiling (Abidi et al., 2008; Gonçalves et al., 2014). Interestingly, KDM5C has been implicated in other neurological abnormalities, including ID caused by mutations in *ARX* (Poeta et al., 2013), autism spectrum disorder (ASD) (Adegbola et al., 2008; Gonçalves et al., 2014), Huntington's disease (Vashishtha et al., 2013), and cerebral palsy (McMichael et al., 2015), suggesting that it may be a critical regulator of brain development and function. *KDM5C* is ubiquitously expressed, with the highest levels observed in brain and skeletal muscle in human (Jensen et al., 2005). In the mouse brain, *Kdm5c* is broadly expressed in areas relevant to cognitive and emotional behaviors such as the prefrontal cortex, hippocampus, and amygdala (Xu et al., 2008). However, the role of KDM5C in the central nervous system remains elusive.

The evolutionary conservation of the chromatin machinery and the genetic nature of the diseases make mice an amenable model for investigating brain disorders associated with mutations in genes encoding chromatin regulators. For example, impaired cognitive function in Rubinstein-Taybi syndrome was recapitulated in mice lacking the histone acetyltransferase gene *Crebbp* (Oike et al., 1999), and Kleefstra syndrome was modeled by targeting *Ehmt1*, the histone H3K9 methyltransferase gene (Schaefer et al., 2009). Deletion of murine *Kmt2d*, an Mll family H3K4 methyltransferase associated with Kabuki syndrome, results in craniofacial dysmorphism and cognitive deficits (Bjornsson et al., 2014). However, no animal model of a human disorder associated with mutations in a histone methylation "eraser" gene has been reported, hindering understanding of the dynamic regulation of histone modification in normal and diseased brains, and the development of potential therapies. We therefore generated *Kdm5c*-knockout (*Kdm5c*-KO) mice to test the hypothesis that loss of Kdm5c function is causal to XLID, to explore the underlying cellular and molecular mechanisms, and to investigate how removal of H3K4me3 by Kdm5c plays a role in the brain.

RESULTS

We disrupted *Kdm5c* function in mice through targeted elimination of exons 11 and 12, which encode its enzymatic domain (Figures S1A–S1C). This knockout strategy is predicted to generate a mutant *Kdm5c* gene encoding an RNA transcript with an in-frame deletion of exons 11 and 12. Nonetheless, the predicted mutant Kdm5c protein is barely detectable in the knockout, and the estimated level of expression is less than 5% of the WT Kdm5c protein level (Figure S1D; data not shown). The *KDM5C* gene is X-linked in humans and mice, and affected human individuals are predominantly male; thus, we focused our analyses on male hemizygous animals, namely *Kdm5c*-knockout mice (−/y, KO) and their WT littermates (+/y, WT). We found that *Kdm5c*-KO mice exhibited smaller body size and reduced body weight (Figure 1A; $p < 0.005$ Student's t test; Figure S1E), which is reminiscent of shorter stature in ~60% of affected individuals (Abidi et al., 2008; Jensen et al., 2005). Despite their reduced body weight, *Kdm5c*-KO male mice are generally in good health and are fertile.

Kdm5c-KO Mice Exhibit Abnormal Social Behavior, Including Aggression, and Impaired Learning and Memory

We next investigated adaptive behaviors that are frequently compromised in XLID patients. Using the resident-intruder paradigm, we examined whether KO mice display elevated aggression, which is reported in one-third of XLID patients with mutated *KDM5C*. *Kdm5c*-KO mice were dramatically more aggressive than WT littermates. Specifically, the latency of the first attack to the intruder mouse was significantly shorter for *Kdm5c*-KO than WT mice (KO: 12.7 ± 2.4 s, n = 13; WT: 37.6 ± 9.2 s, n = 13; $p < 0.05$, Student's t test; Figure 1B). The aggressive behavior of the KO mice would be categorized as maladaptive since they often showed little or no interest in social exploration (e.g., dorsal sniffing) prior to physical attacks and made shorter pauses between attack episodes (Movies S1 and S2). In fact, some *Kdm5c*-KO mice attacked the intruder mouse so viciously in some sessions that we had to separate them abruptly to protect the stimulus mice, leading to different trial lengths; therefore, number of attacks/bites could not be measured. Serum testosterone levels were elevated in *Kdm5c*-KO mice, although the difference was marginally non-significant (KO: 53.9 ± 13.4 ng/dl, n = 7; WT: 28.2 ± 4.2, n = 8; $p = 0.07$, t test; Figure S1F), suggesting that elevated aggression of *Kdm5c*-KO mice might involve changes in testosterone level in addition to altered neural circuitry.

To investigate social behaviors of *Kdm5c*-KO mice in a neutral environment, we employed the three-chamber social approach and memory tests (Silverman et al., 2010). While WT mice spent significantly more time exploring the stimulus mouse than an inanimate object, *Kdm5c*-KO mice spent similar time between the two (WT: 126.4 ± 13.6 s on stimulus mouse versus 30.9 ± 5.0 s on object, n = 16, $p < 0.0001$; KO: 87.1 ± 13.2 s on stimulus mouse versus 55.9 ± 12.5 s on object, $p = 0.14$; paired t test in both cases; Figure 1C). The absence of preference for a conspecific is not likely attributable to a sensory discrimination defect, as both WT and *Kdm5c*-KO mice preferred the novel over familiar stimulus mouse in the subsequent social memory tests (Figure S1G). These data suggest that *Kdm5c*-KO mice display a reduced motivation for and/or interest in social interaction that is intrinsic and governed by genetically programmed neural circuits (Silverman et al., 2010). This phenotype is consistent with the manifestation of autistic behaviors in some individuals with *KDM5C* mutations (Adegbola et al., 2008).

We then employed the elevated-plus maze paradigm to measure anxiety levels. Interestingly, compared with WT littermates, *Kdm5c*-KO mice spent significantly more time in the open arms of the maze and significantly less time in the closed arms (Figure 1D; $p < 0.05$, Student's t test), suggesting that *Kdm5c*-KO mice have decreased anxiety levels. Of note, in the activity chamber *Kdm5c*-KO mice showed increased locomotor activity during the first 5 min (Figure 1E; $p < 0.05$, Student's t test), but similar activity to WT littermates in subsequent 5 min bins and over the entire 30-min period (Figures 1E and S1H). This suggests that the reduced anxiety phenotype may also manifest

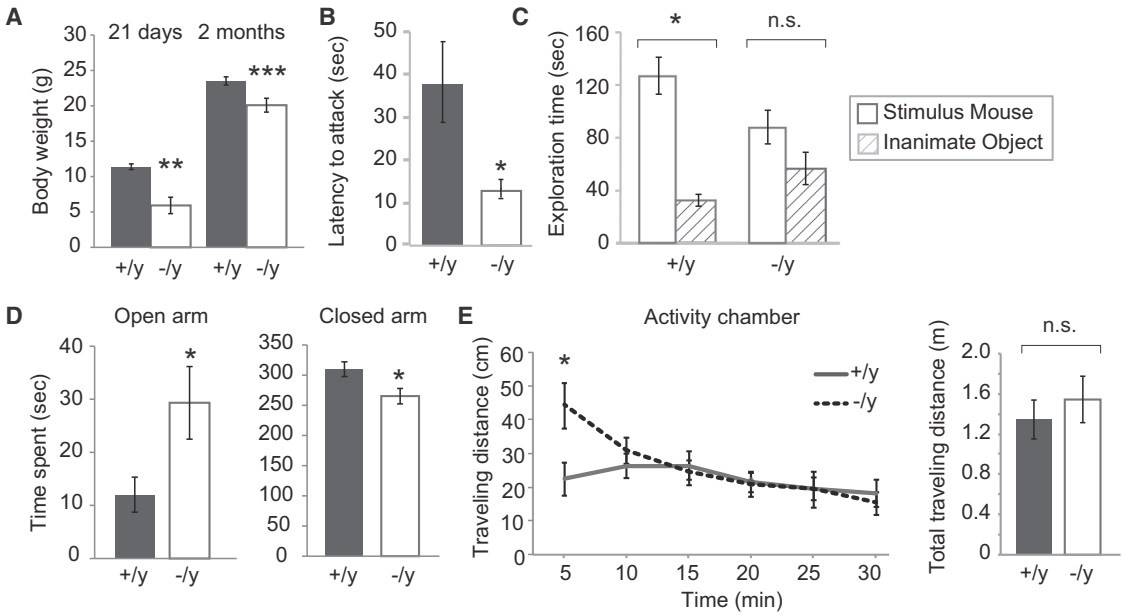

Figure 1. *Kdm5c*-KO Mice Are Small, Aggressive, and Show Social Defects

In the initial behavioral study, nine *Kdm5c*-KO mice (−/y, KO) and nine WT littermates (+/y, WT) were analyzed in a blind fashion. Based on power analysis, additional mice were analyzed for resident-intruder (13 WT, 13 KO) and social approach (16 WT, 14 KO) tests.

(A) Kdm5c-KO mice had a significantly lower body weight at weaning (21 days) and in adulthood.

(B) KO mice showed shorter latencies to attack stimulus mice than WT in the resident-intruder paradigm.

(C) WT but not KO mice spent more time with the stimulus mouse than with an inanimate object (*$p < 0.001$, paired t test separately for WT and KO) in the social approach test.

(D) KO mice spent significantly more time in the open arms and less time in the closed arms in the elevated plus maze anxiety test than WT littermates.

(E) *Kdm5c*-KO mice were more active during the first 5-min period in activity chamber, but showed no difference in any subsequent 5-min bin or overall (30 min).

p values are from Student's t tests unless otherwise noted (*$p < 0.05$, **$p < 0.005$, ***$p < 0.0005$).

as hyperactivity during initial exposure to a novel environment, i.e., disinhibition or "boldness." In the open field test, we did not observe a statistically significant difference between the two genotypes in the time spent in the center, suggesting that reduced anxiety of *Kdm5c*-KO mice is assay dependent (Figure S1I). It has been suggested that behavioral assays, such as elevated plus maze, open field, and light-dark exploration, measure different forms of anxiety, with each being regulated by a set of partially overlapping genes (Turri et al., 2001). Indeed, it is not uncommon that a mutation causes an anxiety phenotype in some tests but not others (van Gaalen and Steckler, 2000).

In order to investigate the cognitive function of *Kdm5c*-KO mice, we first carried out fear conditioning, which is commonly used to assess learning and memory. *Kdm5c*-KO mice showed significantly reduced freezing responses upon exposure to the context or auditory cues, which had been paired with aversive events (foot shock) 24 hr earlier (Figure 2A; $p < 0.005$, Student's t test). The reduced fear response of *Kdm5c*-KO mice was also seen in short-term contextual tests following conditioning in two independent cohorts, suggesting that Kdm5c is required for memory acquisition (Figures S2A and S2B). Decreased freezing behavior is not due to impaired sensory perception, as *Kdm5c*-KO animals showed similar responses to WT littermates in the nociceptive test (Figure 2B).

We also carried out the Morris Water Maze test to characterize spatial learning. Over a 4-day period with four trials daily, *Kdm5c*-KO mice showed a significantly slower decline in latency and longer swimming trajectories to find the platform ($p < 0.01$, repeated-measures ANOVA; Figures 2C and S2C). Poor performance cannot be attributed to swimming deficiency of *Kdm5c*-KO mice because their swimming speed was comparable to that of WT littermates (Figure 2D). Taken together, these behavioral data demonstrate that Kdm5c is required for the normal development and/or execution of adaptive, emotional, and cognitive behaviors.

Kdm5c Is Required for Dendritic Arborization and Spine Morphology

To determine whether loss of *Kdm5c* results in behavioral alterations due to changes in overall brain architecture, we performed Nissl staining. We found no gross abnormalities in the cytoarchitecture of the adult *Kdm5c*-KO cerebral cortex, hippocampus, or amygdala (6 months old; Figure 3A), which are crucial for learning and adaptive behaviors. Further examination of the neocortex using dendritic marker Map2 and neuronal subtype-specific markers Ctip2, Satb2, Gad1/2, Nos1, and Pvalb did not reveal overt differences between WT and *Kdm5c*-KO mice (Figure S3A). These results suggest that *Kdm5c* is dispensable for gross morphogenesis of key brain areas.

Abnormal dendritic arborization and spine morphology have been implicated as a cellular basis of human ID and its mouse

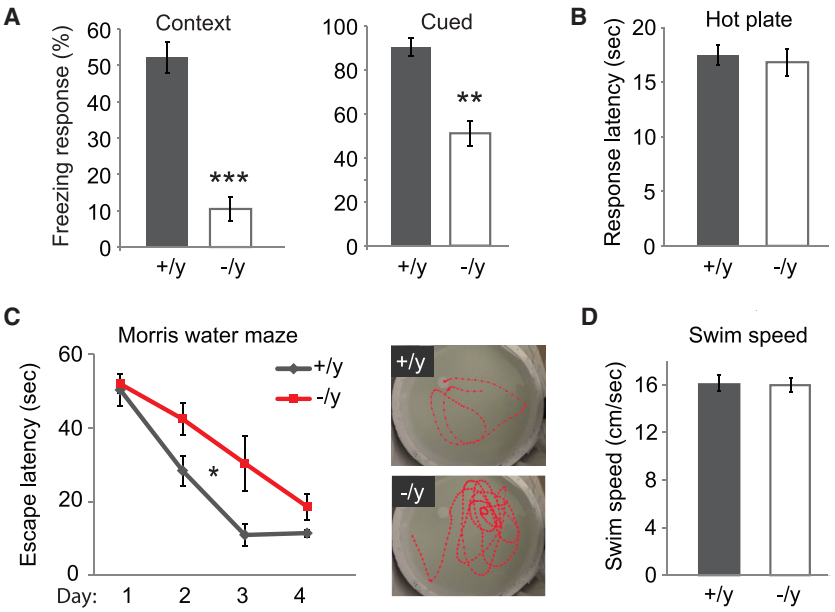

Figure 2. Learning and Memory Deficiency of *Kdm5c*-KO Mice

(A) In both contextual and cued fear conditioning, *Kdm5c*-KO mice showed a significantly reduced freezing response than WT in 3-min trials.

(B) KO mice showed similar response latency as WT mice in the hot plate test for pain perception.

(C) In the Morris water maze, KO mice took longer than WT to reach the hidden platform (*$p < 0.01$, repeated-measures ANOVA). (Right panels) Representative swim trajectory in the third trial on the third testing day.

(D) KO mice showed no defect in swimming speed.

Mean ± SEM in all panels. p values (*$p < 0.05$, **$p < 0.005$, ***$p < 0.0005$) are from Student's t tests unless noted.

models (Penzes et al., 2011). We have previously shown that *Kdm5c* is required for full dendritic arborization in rat cerebellar granular neurons in culture (Iwase et al., 2007), but the role of Kdm5c in dendritic growth in vivo and in spine morphogenesis remains unknown. The basolateral amygdala (BLA) plays a central role in perception and modulation of emotion, including fear and aggression (Davis and Shi, 2000). Since *Kdm5c*-KO mice showed abnormalities in aggression and fear memory (Figures 1 and 2), we first determined whether dendritic growth in the BLA is affected by Kdm5c deficiency. Golgi staining followed by Sholl analysis showed that *Kdm5c*-KO pyramidal neurons had significantly fewer dendritic intersections selectively in the concentric circles that are distant from the soma (Figures 3B and 3C; 150–390 μm, two-way ANOVA, $p < 0.001$), suggesting that extension and/or branching of dendrites are affected. Indeed, dendrites of BLA pyramidal neurons showed significantly reduced total length (Figure 3D; Student's t test, $p < 0.0005$) in the BLA of *Kdm5c*-KO mice compared with that of WT littermates. Moreover, a reduced spine density, approximately 45% of WT, was evident from proximal to distal segments of dendritic branches in *Kdm5c*-KO neurons (Figure 3E). Many dendritic spines on *Kdm5c*-KO neurons were noticeably thinner than those of WT neurons and lacked mature mushroom-like morphology (Figure 3B, lower).

To determine whether these cellular defects are specific to the BLA, we examined the morphology of pyramidal neurons in the motor cortex of *Kdm5c*-KO mice and found a slight (9%) but significant reduction of spine density (Student's t test, $p < 0.05$; Figures S3B–S3D). However, we did not find any changes in dendritic arborization in this particular brain area (Figures S3E and S3F). Taken together, these data demonstrate that Kdm5c plays a role in the morphogenesis of dendrites and dendritic spines in vivo, with a brain region-dependent sensitivity to the loss of Kdm5c.

Kdm5c-KO Brains Show Altered Transcription Profiles

Kdm5c has been shown to repress neuron-specific genes in non-neuronal cells (Tahiliani et al., 2007) and Myc target genes in mouse embryonic stem (mES) cells (Outchkourov et al., 2013). However, the genome-wide role of Kdm5c in the brain remains unexplored. We therefore sought to determine the impact of Kdm5c loss on the transcriptome of the amygdala (AMY) and frontal cortex (FC) of adult mice, areas relevant for the *Kdm5c*-KO behavioral phenotype (Figures 1, 2, S1, and S2) and where we had observed defects in spine morphogenesis (Figures 3 and S3). RNA-seq identified a comparable number of differentially expressed genes in *Kdm5c*-KO amygdala (upregulated: 361, downregulated: 214) and frontal cortex (up: 440, down: 252) compared with WT brain tissues ($p < 0.01$; Figure 4A; Table S1). The larger number of upregulated genes than downregulated genes is consistent with the enzymatic activity of Kdm5c, which removes the active chromatin marks H3K4me2/3. The overlap of differentially regulated genes between the amygdala and the frontal cortex (98 upregulated and 21 downregulated genes) was relatively small. The median changes of gene expression were modest, ranging from 1.40- to 1.52-fold (Figure 4B), suggesting that Kdm5c has a role in fine-tuning expression of hundreds of genes.

To explore the biological significance of the altered gene expression program in *Kdm5c*-KO brain areas, we used LR path gene set enrichment program (Kim et al., 2012) to define the gene ontologies (GOs) that were significantly mis-regulated in at least one brain area (false discovery rate [FDR] < 0.015). Cluster analysis of these GO terms indicated that the two brain areas of the KO mice display largely distinct patterns of transcriptional alteration. We defined four main classes based on the hierarchical clustering of upregulation or downregulation of GO terms in the amygdala and in the frontal cortex (Figure 4C; Table S2). Interestingly, categories that were downregulated in KO amygdala but unchanged in KO frontal cortex (class I) are highly relevant for neuronal differentiation, neuron-projection development, and synapses (Figure 4C), which is consistent with the dendritic growth defect in *Kdm5c*-KO BLA (Figure 3) but not motor cortex (Figure S3). Consistent with the more severely reduced spine density in the amygdala, when we

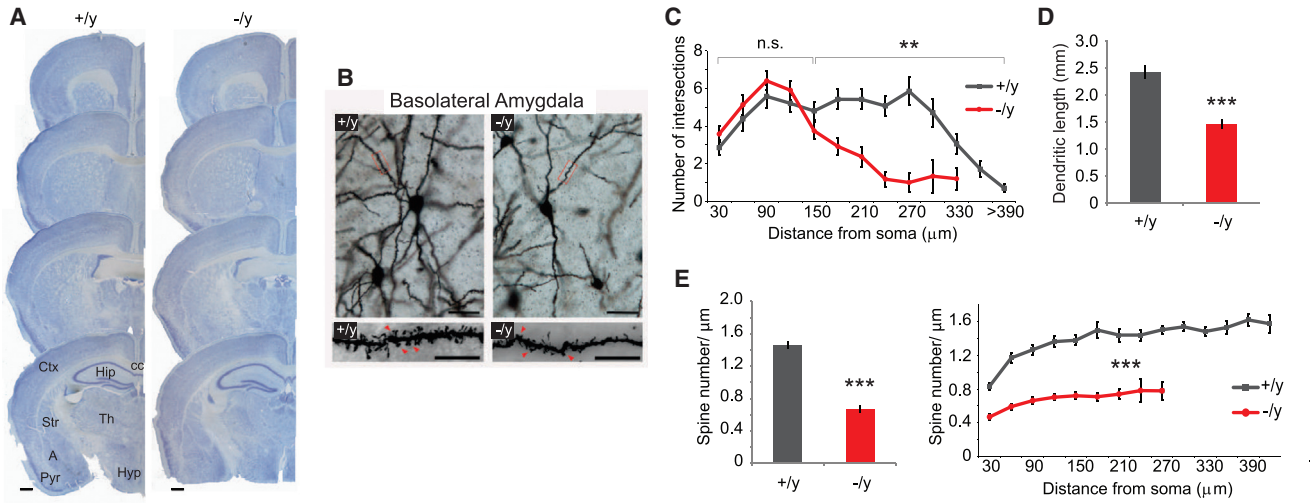

Figure 3. Loss of *Kdm5c* Resulted in Defects in Dendritic Arborization and Spine Morphology In Vivo

(A) Nissl staining of adult WT and *Kdm5c*-KO coronal brain sections. Gross morphology of the brain was preserved in KO mice. A, amygdala; cc, corpus callosum; Ctx, cerebral cortex; Hip, hippocampus; Hyp, hypothalamus; Pyr, pyriform cortex; Str, striatum; Th, thalamus. Scale bars represent 500 μm.

(B) Representative BLA pyramidal neurons visualized by Golgi staining. Scale bars represent 20 μm (upper) and 3 μm (lower). Bifurcated and mushroom-shaped dendritic spines (red arrowheads in WT) were less evident in KO neurons. Throughout the study, 20 neurons per genotype from adult KO and WT littermates (n = 4 per genotype) were analyzed in a blind fashion.

(C) KO neurons had fewer intersections in outer concentric circles in the BLA (left, 150–390 μm, two-way ANOVA, $^{**}p < 0.05$).

(D) Reduced dendritic length of BLA pyramidal neurons in KO mice.

(E) BLA pyramidal neurons of KO showed significantly lower spine density (left), which was seen from proximal to distal segments ($^{***}p < 0.0005$, two-way ANOVA, right).

Mean ± SEM in all panels. p values ($^{*}p < 0.05$, $^{**}p < 0.005$, $^{***}p < 0.0005$) are from Student's t tests unless noted.

used "Reactome," a curated biological pathway database (Croft et al., 2014), synaptic pathways such as "Glutamate Neurotransmitter Release Cycle" and "Nicotinic acetylcholine receptors" are downregulated in the KO amygdala but not in the frontal cortex (Figure S4A). Categories that were upregulated in *Kdm5c*-KO amygdala but unchanged in the frontal cortex include GO terms related to cilia (Figure 4C, class III), which play an important role in neurodevelopment (Louvi and Grove, 2011). GOs showing upregulation in the amygdala and downregulation in the frontal cortex include behavior-related ontologies such as response to amphetamine (Figure 4C, class IV). These data suggest that Kdm5c loss leads to different functional consequences depending on the brain area.

To determine whether genes associated with neurodevelopmental disorders significantly overlap with the mis-regulated genes in *Kdm5c*-KO brain, we performed LR path analyses using curated lists of genes that are associated with IDs (Gardiner, 2015), ASDs (Basu et al., 2009), and schizophrenia (Fromer et al., 2014). Although many of these genes overlapped with mis-regulated genes in the KO brains, we did not find statistically significant enrichment in either the amygdala or the frontal cortex ($p = 0.37 \sim 0.93$; Table S3). Collectively, mis-regulation of hundreds of genes involved in neurodevelopment rather than known human disorder genes is likely instructive to KDM5C deficiencies.

Elevated aggression (Figure 1B) and a trend of higher testosterone levels (Figure S1F) in *Kdm5c*-KO mice prompted us to examine the possibility that altered androgen levels may mediate some of the effects of *Kdm5c* loss on the brain transcriptome. We examined the expression levels of 979 annotated androgen-responsive genes (ARGs) (Jiang et al., 2009) as a group in WT and *Kdm5c*-KO amygdala and frontal cortex, and detected no difference as a whole (Figure S4B). However, we did identify a statistically significant enrichment of ARGs in the list of mis-regulated genes in the amygdala and the frontal cortex (Figure S4C; Table S4). Enrichment was more pronounced in up-regulated genes (chi-square test, $p < 4.0 \times 10^{-23}$) than in down-regulated genes ($p < 1.4 \times 10^{-3}$), which is consistent with a higher testosterone level in *Kdm5c*-KO serum. These results suggest that the higher testosterone level in *Kdm5c*-KO mice, albeit marginally non-significant, may elicit upregulation of ARGs in *Kdm5c*-KO brain and, in turn, behavioral phenotypes.

Molecular Mechanisms of Kdm5c-mediated Gene Regulation in Neurons

To gain insight into the molecular mechanisms underlying Kdm5c function in post-mitotic neurons, we performed integrated functional genomic analysis of dissociated cortical neurons isolated from the forebrain (which gives rise to brain tissues including the cortex and amygdala) at E16.5 and harvested after 10 days of in vitro culture. This culture system allows us to investigate gene regulation by Kdm5c in a relatively homogenous neuronal population, with minimal glial contamination (Brewer et al., 1993).

We first determined sites of Kdm5c recruitment in post-mitotic neurons by chromatin immunoprecipitation coupled with deep sequencing (ChIP-seq) using an anti-Kdm5c antibody. Our

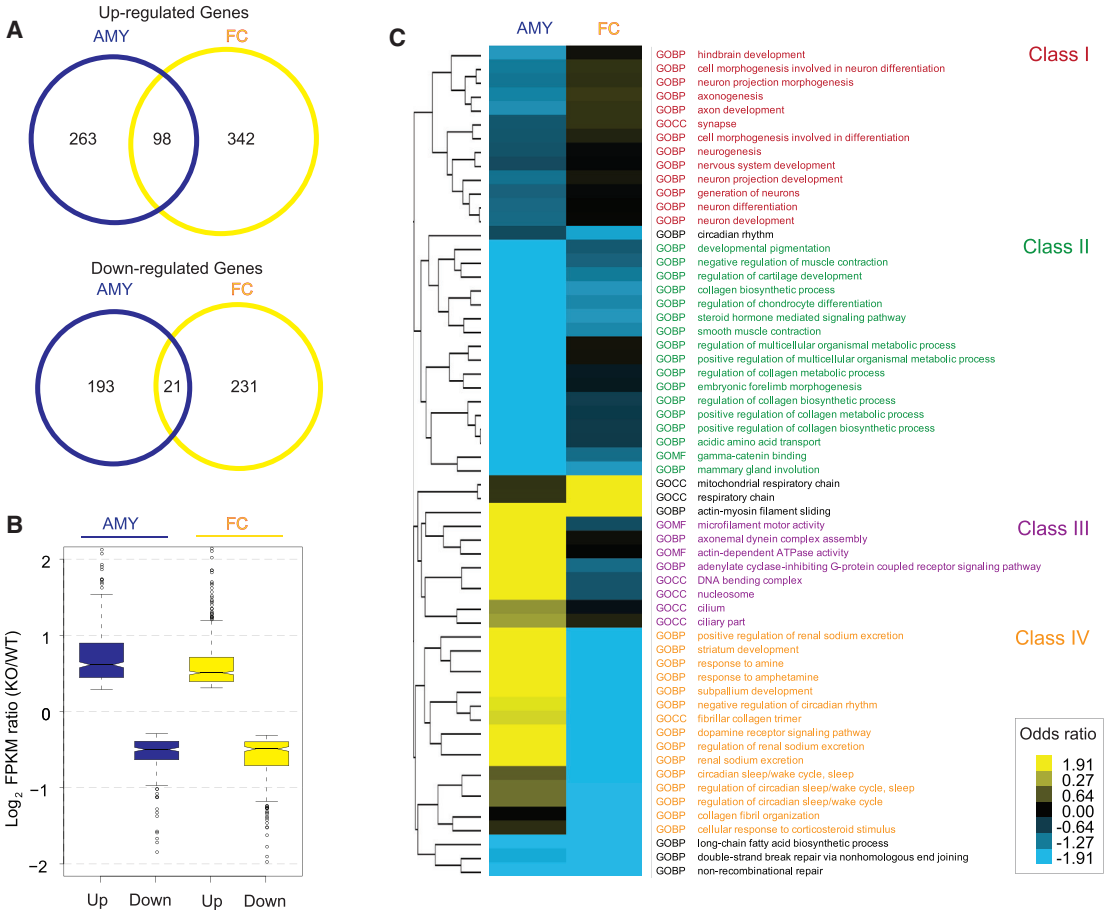

Figure 4. Altered Transcription Profiles in *Kdm5c*-KO Brain Tissues

RNA-seq data were obtained from the amygdala (AMY) and the frontal cortex (FC) of three adult mice for each genotype.

(A) Differentially expressed (DE) genes between WT and *Kdm5c*-KO brain ($p < 0.01$). AMY and FC show a modest overlap.

(B) KO/WT ratio of expression levels of DE genes. Box signifies the upper and lower quartiles, the interquartile range (IQR), with the median represented by a short black line. Whiskers, 1.5 × IQR.

(C) LR path analysis of mis-regulated GO categories followed by clustering (FDR < 0.015). The odds ratio for enrichment is shown. Yellow and blue indicate upregulation and downregulation in KO compared with WT, respectively. Four major classes (I to IV) represent differential alteration patterns between AMY and FC.

ChIP-seq analysis identified 6,728 high-confidence Kdm5c peaks after subtracting peaks found in the *Kdm5c*-KO neurons, which constitute non-specific and low-confidence peaks. We found that 48% and 16% of Kdm5c peaks fall within gene promoters and enhancers, respectively, which represent a significant enrichment at these two functional elements (Figures 5A and S5A). The vast majority of Kdm5c peaks (93%) are found within 500 bps of DNase I hypersensitivity sites (DHSs; Figure S5B), a marker of open chromatin and active cis-regulatory elements (obtained from E14.5 and P56 mouse brains; Neph et al., 2012), suggesting that Kdm5c modulates transcription of active genes. At promoters, Kdm5c shows a pronounced peak at the transcription start site (TSS; Figures 5B and S5C). We observed a detectable but significantly lower Kdm5c ChIP signal in *Kdm5c*-KO neurons (Figures 5B, S5C, and S5H), which is probably attributable to a trace amount of Kdm5c lacking the enzymatic domain (Figure S1D).

We noted that Kdm5c peaks often coincide with CpG islands (Figures 5B and S5C). Genome-wide assessment reveals that the majority of Kdm5c-bound promoters (94%) contain a CpG island, representing a significant enrichment over the genomic average (Figure 5C; $p < 1 \times 10^{-26}$, chi-square test). Kdm5c occupies 26% of CpG-containing promoters but only 2% of non-CpG promoters (Figure S5D). CpG island-regulated genes encode both highly expressed housekeeping genes and tissue-specific genes, and their promoters are extensively decorated with H3K4me3 (Deaton and Bird, 2011). Indeed, both mRNA and promoter H3K4me3 levels are significantly higher for CpG island-regulated genes compared with non-CpG genes in neurons (Figure S5E). Consistently, we found that Kdm5c levels at target promoters are positively correlated with expression levels of corresponding genes (Figure S5F), and Kdm5c-bound genes are enriched for middle and highly expressed genes (Figure S5G). Even lowly expressed Kdm5c-target genes

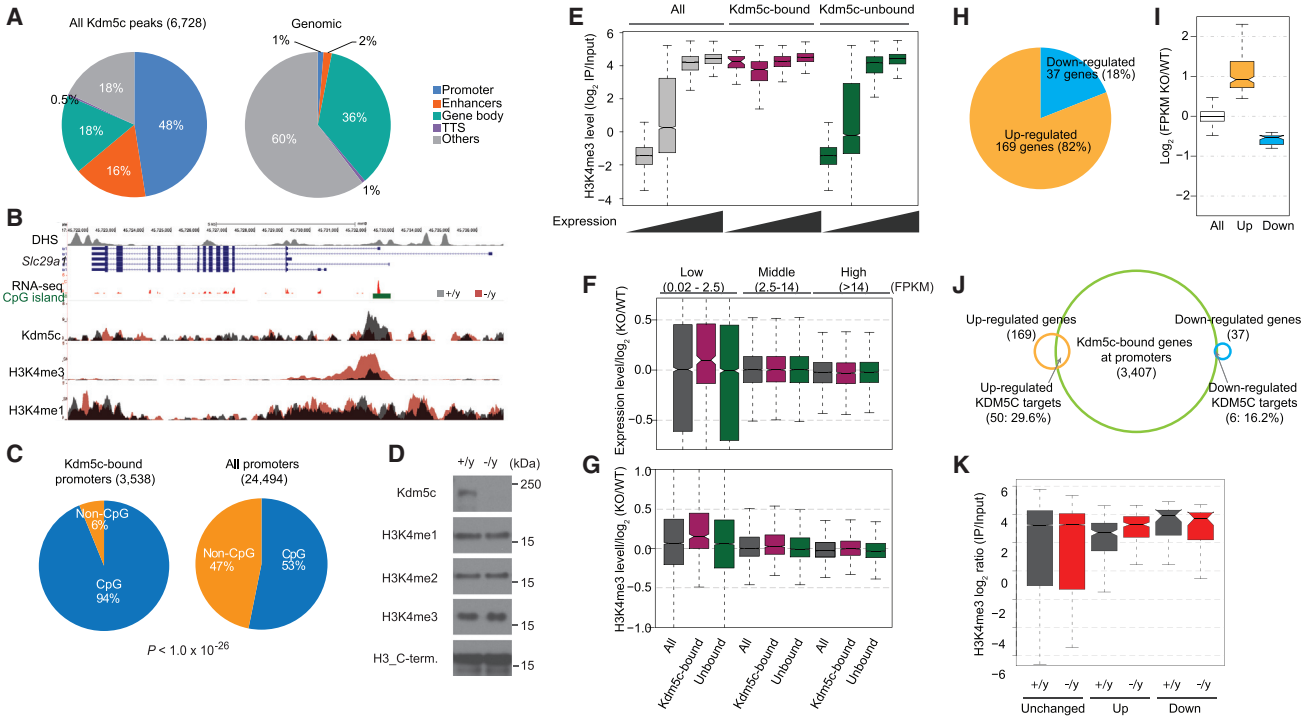

Figure 5. Kdm5c Is Recruited to CpG Promoters with High H3K4me3 in Post-mitotic Neurons and Represses Transcription

ChIP-seq and RNA-seq were performed on two biological replicates of WT and *Kdm5c*-KO neurons.

(A) Enrichment of high-confidence Kdm5c peaks in promoter and enhancer regions (left) compared with genomic fractions (right). Promoter, ± 1.5 kb of TSS; enhancers, ± 2.0 kb of intergenic DNaseI hypersensitive sites (DHS) of E14.5 and adult brains (Neph et al., 2012); TTS, ± 1.0 kb of transcription termination sites.

(B) UCSC browser shot of Kdm5c, H3K4me3, and H3K4me1 across the Kdm5c-bound locus *Slc29a1* (gray, WT; red, KO). RNA-seq in WT neurons is shown in red; CpG island position is indicated in green.

(C) Most Kdm5c-bound promoters harbor CpG islands (left), which represents strong enrichment over the genomic average (right) ($p < 1.0 \times 10^{-26}$, chi-square test).

(D) Western blot analysis shows that global H3K4me levels are not altered in *Kdm5c*-KO neurons. Representative image is from two biological replicates.

(E) WT neurons were used to divide genes into four groups (with approximately equal numbers of genes) according to expression level. Kdm5c-bound promoters with low expression levels show significantly higher H3K4me3 levels than unbound genes with the same expression levels.

(F and G) Expression and H3K4me3 changes in *Kdm5c*-KO neurons. WT neurons were used to divide genes into three groups (with approximately equal numbers of genes) according to expression level. Low-expressed Kdm5c-target genes showed the most noticeable increase in expression (median: ~7% increase, $p = 1.4 \times 10^{-8}$, Wilcoxon signed rank test) and H3K4me3 (median: ~12% increase, $p < 2.2 \times 10^{-16}$, Wilcoxon signed rank test) in KO neurons.

(H) 206 differentially expressed (DE) genes in *Kdm5c*-KO neurons identified by RNA-seq ($p < 0.025$).

(I) Expression level fold change of unchanged and DE genes in KO neurons compared with WT.

(J) Overlap of Kdm5c-bound promoters with DE genes from KO/WT.

(K) Upregulated and downregulated genes showed significantly higher or lower H3K4me3 levels in *Kdm5c*-KO neurons, respectively ($p < 2.0 \times 10^{-5}$ in Wilcoxon signed rank test).

In box plots, box signifies the upper and lower quartiles, the interquartile range (IQR), with the median represented by a short black line. Whiskers, 1.5 × IQR.

are unexpectedly marked with high H3K4me3 (Figure 5E), suggesting that CpG islands and high H3K4me3 are the primary chromatin signatures that recruit Kdm5c.

KDM5C mediates demethylation of H3K4me3 and H3K4me2 (Iwase et al., 2007; Tahiliani et al., 2007), which are generally associated with actively transcribed genes. In neurons, global levels of H3K4me1, H3K4me2, or H3K4me3 are comparable in WT and *Kdm5c*-KO neurons (Figure 5D), suggesting that Kdm5c is not a global regulator of H3K4 methylation. We postulated that Kdm5c plays a region-specific role, acting to downregulate gene transcription by removing H3K4me3 from actively transcribed promoters. To test this hypothesis, we generated RNA-seq and H3K4 methylation (H3K4me3, H3K4me1) ChIP-seq data from WT and *Kdm5c*-KO neurons.

To analyze the impact of Kdm5c promoter binding, we compared mRNA and H3K4me3 levels of all Kdm5c-bound genes in WT and *Kdm5c*-KO neurons and, surprisingly, did not find any significant difference (data not shown). However, when we grouped genes based on their mRNA levels, we noticed significant upregulation of lowly expressed Kdm5c target genes in *Kdm5c*-KO relative to WT neurons (Figure 5F; median: ~7% increase, $p = 1.4 \times 10^{-8}$, Wilcoxon signed rank test). Similarly, H3K4me3 levels at the lowest expressed Kdm5c targets (±1.5 kb of TSS) were increased in *Kdm5c*-KO neurons (Figure 5G; median: ~12% increase, $p < 2.2 \times 10^{-16}$, Wilcoxon signed rank test). Plotting the distribution of H3K4me3 around the TSS for these different groups demonstrated that low, but not middle or high, expressed Kdm5c targets showed an

increase in H3K4me3 at promoters (Figure S5H; $p < 0.05$, Student's t test). In contrast, H3K4me1 levels downstream of the TSS were higher in KO regardless of gene expression levels (Figure S5H). These data indicate that Kdm5c primarily acts as a transcriptional co-repressor when bound at promoters and that lowly expressed genes are more sensitive to the loss of Kdm5c. The absence of significant mis-regulation of the majority of Kdm5c-bound genes suggests that Kdm5c mainly plays a fine-tuning role, which is consistent with our brain tissue RNA-seq (Figure 4). Although we did not observe a compensatory increase in mRNA levels of other Kdm5 family members in *Kdm5c*-KO neurons (Figure S5I) or brain tissues (Figure S5J), functional redundancy may also explain the minimal effects of *Kdm5c* loss on genes with higher expression levels.

RNA-seq analysis from the neuronal cultures identified 169 upregulated and 37 downregulated genes in *Kdm5c*-KO neurons compared with WT (Figure 5H; $p < 0.025$; Table S5). We found a considerable overlap of the differentially expressed genes in cultured neurons with those identified from brain tissues (Figure S5K). We validated a panel of upregulated genes, including genes that are also upregulated in the brain tissues, using quantitative RT-PCR (qRT-PCR) (Figure S5L). Upregulated genes that are common to both cultured neurons and brain tissue likely represent Kdm5c-regulated events specific to neurons rather than other cell types present in brain tissue. Similar to brain tissues, the magnitude of the gene expression changes in cultured neurons was modest (Figure 5I; upregulated genes: 1.88-fold; downregulated genes: 1.44-fold). When we integrated RNA-seq and Kdm5c ChIP-seq data from cultured neurons, we found high-confidence Kdm5c peaks at the promoters of 29.6% of upregulated genes but only 16.2% of downregulated genes (Figure 5J). Significantly upregulated or downregulated genes in *Kdm5c*-KO neurons showed an increase or decrease of H3K4me3, respectively, both genome-wide (Figure 5K) and at specific loci (Figures 5B and S5C). These genome-wide data identified mechanisms of Kdm5c-mediated gene repression, which may account for mis-regulation of genes in vivo that are closely associated with dendritic and behavioral deficits.

DISCUSSION

We have generated and characterized a mouse model of ID caused by the loss-of-function of a histone demethylase. Importantly, *Kdm5c*-KO mice recapitulate key cognitive, adaptive, and social abnormalities seen in patients with *KDM5C* mutations, including increased aggression, decreased anxiety and social behavior, and defects in learning and memory (Figures 1 and 2).

We identified a significant reduction in dendritic arborization and spine density in the BLA (Figures 3B–3E), a region known to be important for the formation of fear memory and for aggressive behavior (Davis and Shi, 2000). Spine density in the BLA has previously been linked to anxiety and cognitive deficits (Leuner and Shors, 2013), suggesting that these alterations may contribute to the behavioral phenotypes. In contrast, spine density was slightly reduced in the cortex of *Kdm5c*-KO mice, whereas dendritic arborization was unaffected (Figure S3). Different changes in gene expression were identified in *Kdm5c*-KO amygdala and cortical brain tissues (Figure 4). Differential sensitivity to Kdm5c loss between brain areas in both cellular phenotypes and gene expression levels emphasizes the importance of future investigation into brain region-specific roles of Kdm5c. We are currently carrying out a systematic analysis to localize the anatomical substrates for individual behavioral phenotypes by genetically deleting *Kdm5c* in discrete brain locations and in specific cell types.

Our ChIP-seq and RNA-seq analyses in cultured neurons have provided molecular insights into how Kdm5c might regulate neuronal function. ChIP-seq identified Kdm5c at gene promoters characterized by the presence of CpG islands and high H3K4me3 (Figures 5C, S5D, and S5E), raising the possibility that these are the primary determinants for Kdm5c recruitment to promoters in neurons. The effect of Kdm5c loss on gene expression is more pronounced at genes with low expression (Figure 5F), which are marked by unexpectedly high H3K4me3 levels in WT neurons (Figure 5E). High H3K4me3 at genes with low expression is a hallmark of poised chromatin, often found at genes required to undergo rapid activation (Margaritis and Holstege, 2008). It would be interesting to investigate the role of Kdm5c at poised genes, such as neuronal activity-dependent genes (Saha et al., 2011).

Loss of Kdm5c causes both upregulation and downregulation of gene expression, but a higher percentage of genes are upregulated upon *Kdm5c* loss in both brain tissues and cultured neurons (Figures 4A and 5H), indicating that Kdm5c mainly functions as a transcriptional repressor. A recent report suggested that Kdm5c can also act as a transcriptional activator, possibly by impacting enhancer function in mES cells (Outchkourov et al., 2013). We note that a considerable number of genes showed downregulation in *Kdm5c*-KO neurons (Figures 4A and 5H) and that Kdm5c binds to enhancers (Figure 5A). However, whether downregulation of these genes is a result of loss of Kdm5c at enhancers that control their expression and, indeed, whether Kdm5c regulates enhancer activities in neurons remain to be investigated.

We found multiple key pathways that play essential roles in the development and function of neuronal circuitry to be aberrantly expressed in the *Kdm5c*-KO brain (Figure 4C). Importantly, the differential severity of dendritic phenotypes between amygdala and cortex correlates with the downregulation of neurodevelopmental pathways, lending support to the hypothesis that these downregulated genes contribute to the dendritic morphologies in *Kdm5c*-KO brains (Figure 4). Other mis-regulated pathways include "Cilium," "Dopamine receptor signaling pathway," "Glutamate neurotransmitter release cycle," "Nicotinic acetylcholine receptors," and "GABA receptor activation" (Figures 4 and S4A; Table S2), suggesting that the loss of Kdm5c may have impact on cilia function and diverse neurotransmitter systems in a brain area-dependent manner. Thus, our transcriptome analyses provide a useful resource for future investigations to determine the downstream effector genes responsible for phenotypic outcomes in this unique mouse model of ID.

Although the magnitude of gene mis-regulation in *Kdm5c*-KO neurons is modest (Figures 4B and 5I), it is possible that an accumulation of small changes in multiple pathways may collectively contribute to the observed behavioral and cellular abnormalities.

Alternatively, specific deficits may be attributable to a single receptor-mediated pathway in a brain region- and/or circuitry-specific fashion. In addition, it remains to be determined whether there is a critical period for Kdm5c function during development. Therefore, it will be important in the future to employ pharmacological and genetic approaches to determine (1) whether the behavioral and cellular deficits originate during development and (2) the functional significance of Kdm5c target genes for their contributions to the phenotypes associated with the loss of *Kdm5c*. In conclusion, our mouse model of XLID caused by mutations in *KDM5C* provides insights into the fundamental mechanisms by which histone methylation dynamics sculpt the neuronal network and a foundation for strategizing future XLID therapies.

EXPERIMENTAL PROCEDURES

Gene targeting was carried out in a 129-derived mES cell line. After germline deletion of floxed segment using B6.C-Tg(CMV-cre)1Cgn/J mice (The Jackson Laboratory), the knockout allele was maintained on a C57BL/6J background (The Jackson Laboratory) with more than nine generations of backcrossing, thereby eliminating 129 genetic background. To minimize phenotypic variability due to heterogeneous genetic background, we compared F1 littermates generated from breeding between a heterozygous KO female on the C57BL/6J background and a WT 129S1/SvImJ male (The Jackson Laboratory) throughout the present study (Silva et al., 1997). Behavioral paradigms were performed according to standard protocols and in a blind fashion. Morphological analyses of dendrites were carried out as described previously (Shmelkov et al., 2010). RNA-seq libraries were prepared from the frontal cortex and the amygdala of adult (3 to 6 months) mice and from cultured neurons after 9–10 days in vitro, according to method described previously (Agarwal et al., 2015). RNA-seq and ChIP-seq libraries were sequenced on an Illumina HiSeq 2000 system; resulting reads were mapped and analyzed as described in supplementary methods.

Animals

Animal procedures were approved by institutional animal care and use committees of Boston Children's Hospital (13-08-2474R), Washington State University (04298), and the University of Michigan (PRO00004174).

ACCESSION NUMBERS

RNA-seq and ChIP-seq data are available in the Gene Expression Omnibus under accession number GEO: GSE61036.

SUPPLEMENTAL INFORMATION

Supplemental Information includes Supplemental Experimental Procedures, five figures, five tables, and two movies and can be found with this article online at http://dx.doi.org/10.1016/j.celrep.2015.12.091.

AUTHOR CONTRIBUTIONS

S.I., J.X., and Y.S. conceived the project. S.I., E.B., S.A., A.I.B., C.C., K.Y.K., and J.X. designed experiments. S.I., E.B., S.A., A.I.B., H.I., G.S.T., T.K., C.N.V., G.L., and A.T. performed experiments. S.A. analyzed genomics data, and L.G., B.E., and M.A.S. assisted in the analysis. G.S.T. performed Nissl and IF analysis of cerebral cortex markers. S.I., E.B., J.X., A.I.B., S.A., and Y.S. wrote the manuscript.

CONFLICTS OF INTEREST

Y.S. is a co-founder of Constellation Pharmaceutical, Inc., and a member of its scientific advisory board.

ACKNOWLEDGMENTS

We thank Dr. Bing Ren for helpful discussions and sequencing of the libraries and Dr. Paola Arlotta for advice and critical reading of the manuscript. We thank Dr. A. Sharpe and M.J. Kim at Brigham & Women's Hospital Transgenic Core Facility for generation of *Kdm5c*-KO mice; H. Liu, K. Yamagata, M. Geigges, and all members of the Shi laboratory for experimental help and helpful discussions; Dr. Barbara Caldarone at Harvard NeuroBehavior Laboratory Core for additional fear conditioning data and earlier behavior studies; Neurodigitech, LLC for Sholl analysis. This work was supported by grants to Y.S. and J.X. (NIH MH096066), Dr. Ren (NIH: RN2-00905), and S.I. (NIH: NS089896). S.I. was collectively supported by Jane Coffin Childs Memorial Fund, Japan Society for the Promotion of Science, and Cooley's Anemia Foundation. E.B. was partially supported by an EMBO long-term Fellowship. A.I.B. was partially supported by the Autism Science Foundation Postdoctoral Fellowship. C.N.V. is supported by an NIH training grant (T32GM07544), "Michigan Predoctoral Training in Genetics." We also acknowledge the Farrehi Family Foundation for their generous support of this research. Y.S. is an American Cancer Society Research Professor.

Received: June 26, 2015
Revised: November 17, 2015
Accepted: December 20, 2015
Published: January 21, 2016

REFERENCES

Abidi, F.E., Holloway, L., Moore, C.A., Weaver, D.D., Simensen, R.J., Stevenson, R.E., Rogers, R.C., and Schwartz, C.E. (2008). Mutations in JARID1C are associated with X-linked mental retardation, short stature and hyperreflexia. J. Med. Genet. *45*, 787–793.

Adegbola, A., Gao, H., Sommer, S., and Browning, M. (2008). A novel mutation in JARID1C/SMCX in a patient with autism spectrum disorder (ASD). Am. J. Med. Genet. A. *146A*, 505–511.

Agarwal, S., Macfarlan, T.S., Sartor, M.A., and Iwase, S. (2015). Sequencing of first-strand cDNA library reveals full-length transcriptomes. Nat. Commun. *6*, 6002.

Basu, S.N., Kollu, R., and Banerjee-Basu, S. (2009). AutDB: a gene reference resource for autism research. Nucleic Acids Res. *37*, D832–D836.

Bjornsson, H.T., Benjamin, J.S., Zhang, L., Weissman, J., Gerber, E.E., Chen, Y.C., Vaurio, R.G., Potter, M.C., Hansen, K.D., and Dietz, H.C. (2014). Histone deacetylase inhibition rescues structural and functional brain deficits in a mouse model of Kabuki syndrome. Sci. Transl. Med. *6*, 256ra135.

Brewer, G.J., Torricelli, J.R., Evege, E.K., and Price, P.J. (1993). Optimized survival of hippocampal neurons in B27-supplemented Neurobasal, a new serum-free medium combination. J. Neurosci. Res. *35*, 567–576.

Brookes, E., Laurent, B., Õunap, K., Carroll, R., Moeschler, J.B., Field, M., Schwartz, C.E., Gecz, J., and Shi, Y. (2015). Mutations in the intellectual disability gene KDM5C reduce protein stability and demethylase activity. Hum. Mol. Genet. *24*, 2861–2872.

Croft, D., Mundo, A.F., Haw, R., Milacic, M., Weiser, J., Wu, G., Caudy, M., Garapati, P., Gillespie, M., Kamdar, M.R., et al. (2014). The Reactome pathway knowledgebase. Nucleic Acids Res. *42*, D472–D477.

Davis, M., and Shi, C. (2000). The amygdala. Curr. Biol. *10*, R131.

Deaton, A.M., and Bird, A. (2011). CpG islands and the regulation of transcription. Genes Dev. *25*, 1010–1022.

Fromer, M., Pocklington, A.J., Kavanagh, D.H., Williams, H.J., Dwyer, S., Gormley, P., Georgieva, L., Rees, E., Palta, P., Ruderfer, D.M., et al. (2014). De novo mutations in schizophrenia implicate synaptic networks. Nature *506*, 179–184.

Gardiner, K. (2015). Intellectual Disability Gene Database. http://gfuncpathdb.ucdenver.edu/iddrc/iddrc/home.php. University of Colorado Denver, IDDRC.

Gonçalves, T.F., Gonçalves, A.P., Fintelman Rodrigues, N., dos Santos, J.M., Pimentel, M.M., and Santos-Rebouças, C.B. (2014). KDM5C mutational

screening among males with intellectual disability suggestive of X-Linked inheritance and review of the literature. Eur. J. Med. Genet. *57*, 138–144.

Iwase, S., and Shi, Y. (2010). Histone and DNA Modifications in Mental Retardation. In Epigenetics and Disease: Pharmaceutical Opportunities (Progress in Drug Research), S.M. Gasser and E. Li, eds. (Springer Basel), pp. 147–174.

Iwase, S., Lan, F., Bayliss, P., de la Torre-Ubieta, L., Huarte, M., Qi, H.H., Whetstine, J.R., Bonni, A., Roberts, T.M., and Shi, Y. (2007). The X-linked mental retardation gene SMCX/JARID1C defines a family of histone H3 lysine 4 demethylases. Cell *128*, 1077–1088.

Jensen, L.R., Amende, M., Gurok, U., Moser, B., Gimmel, V., Tzschach, A., Janecke, A.R., Tariverdian, G., Chelly, J., Fryns, J.P., et al. (2005). Mutations in the JARID1C gene, which is involved in transcriptional regulation and chromatin remodeling, cause X-linked mental retardation. Am. J. Hum. Genet. *76*, 227–236.

Jiang, M., Ma, Y., Chen, C., Fu, X., Yang, S., Li, X., Yu, G., Mao, Y., Xie, Y., and Li, Y. (2009). Androgen-responsive gene database: integrated knowledge on androgen-responsive genes. Mol. Endocrinol. *23*, 1927–1933.

Kim, J.H., Karnovsky, A., Mahavisno, V., Weymouth, T., Pande, M., Dolinoy, D.C., Rozek, L.S., and Sartor, M.A. (2012). LRpath analysis reveals common pathways dysregulated via DNA methylation across cancer types. BMC Genomics *13*, 526.

Kouzarides, T. (2007). Chromatin modifications and their function. Cell *128*, 693–705.

Leuner, B., and Shors, T.J. (2013). Stress, anxiety, and dendritic spines: what are the connections? Neuroscience *251*, 108–119.

Louvi, A., and Grove, E.A. (2011). Cilia in the CNS: the quiet organelle claims center stage. Neuron *69*, 1046–1060.

Luger, K., Mäder, A.W., Richmond, R.K., Sargent, D.F., and Richmond, T.J. (1997). Crystal structure of the nucleosome core particle at 2.8 A resolution. Nature *389*, 251–260.

Margaritis, T., and Holstege, F.C. (2008). Poised RNA polymerase II gives pause for thought. Cell *133*, 581–584.

McMichael, G., Bainbridge, M.N., Haan, E., Corbett, M., Gardner, A., Thompson, S., van Bon, B.W., van Eyk, C.L., Broadbent, J., Reynolds, C., et al. (2015). Whole-exome sequencing points to considerable genetic heterogeneity of cerebral palsy. Mol. Psychiatry *20*, 176–182.

Neph, S., Vierstra, J., Stergachis, A.B., Reynolds, A.P., Haugen, E., Vernot, B., Thurman, R.E., John, S., Sandstrom, R., Johnson, A.K., et al. (2012). An expansive human regulatory lexicon encoded in transcription factor footprints. Nature *489*, 83–90.

Nestler, E.J. (2014). Epigenetic mechanisms of depression. JAMA Psychiatry *71*, 454–456.

Oike, Y., Hata, A., Mamiya, T., Kaname, T., Noda, Y., Suzuki, M., Yasue, H., Nabeshima, T., Araki, K., and Yamamura, K. (1999). Truncated CBP protein leads to classical Rubinstein-Taybi syndrome phenotypes in mice: implications for a dominant-negative mechanism. Hum. Mol. Genet. *8*, 387–396.

Outchkourov, N.S., Muiño, J.M., Kaufmann, K., van Ijcken, W.F., Groot Koerkamp, M.J., van Leenen, D., de Graaf, P., Holstege, F.C., Grosveld, F.G., and Timmers, H.T. (2013). Balancing of histone H3K4 methylation states by the Kdm5c/SMCX histone demethylase modulates promoter and enhancer function. Cell Rep. *3*, 1071–1079.

Penzes, P., Cahill, M.E., Jones, K.A., VanLeeuwen, J.E., and Woolfrey, K.M. (2011). Dendritic spine pathology in neuropsychiatric disorders. Nat. Neurosci. *14*, 285–293.

Poeta, L., Fusco, F., Drongitis, D., Shoubridge, C., Manganelli, G., Filosa, S., Paciolla, M., Courtney, M., Collombat, P., Lioi, M.B., et al. (2013). A regulatory path associated with X-linked intellectual disability and epilepsy links KDM5C to the polyalanine expansions in ARX. Am. J. Hum. Genet. *92*, 114–125.

Ropers, H.H., and Hamel, B.C. (2005). X-linked mental retardation. Nat. Rev. Genet. *6*, 46–57.

Saha, R.N., Wissink, E.M., Bailey, E.R., Zhao, M., Fargo, D.C., Hwang, J.Y., Daigle, K.R., Fenn, J.D., Adelman, K., and Dudek, S.M. (2011). Rapid activity-induced transcription of Arc and other IEGs relies on poised RNA polymerase II. Nat. Neurosci. *14*, 848–856.

Schaefer, A., Sampath, S.C., Intrator, A., Min, A., Gertler, T.S., Surmeier, D.J., Tarakhovsky, A., and Greengard, P. (2009). Control of cognition and adaptive behavior by the GLP/G9a epigenetic suppressor complex. Neuron *64*, 678–691.

Shmelkov, S.V., Hormigo, A., Jing, D., Proenca, C.C., Bath, K.G., Milde, T., Shmelkov, E., Kushner, J.S., Baljevic, M., Dincheva, I., et al. (2010). Slitrk5 deficiency impairs corticostriatal circuitry and leads to obsessive-compulsive-like behaviors in mice. Nat. Med. *16*, 598–602.

Silva, A.J., Simpson, E.M., Takahashi, J.S., Lipp, H.P., Nakanishi, S., Wehner, J.M., Giese, K.P., Tully, T., Abel, T., Chapman, P.F., et al. (1997). Mutant mice and neuroscience: recommendations concerning genetic background. Banbury Conference on genetic background in mice. Neuron *19*, 755–759.

Silverman, J.L., Yang, M., Lord, C., and Crawley, J.N. (2010). Behavioural phenotyping assays for mouse models of autism. Nat. Rev. Neurosci. *11*, 490–502.

Tahiliani, M., Mei, P., Fang, R., Leonor, T., Rutenberg, M., Shimizu, F., Li, J., Rao, A., and Shi, Y. (2007). The histone H3K4 demethylase SMCX links REST target genes to X-linked mental retardation. Nature *447*, 601–605.

Turri, M.G., Datta, S.R., DeFries, J., Henderson, N.D., and Flint, J. (2001). QTL analysis identifies multiple behavioral dimensions in ethological tests of anxiety in laboratory mice. Curr. Biol. *11*, 725–734.

van Bokhoven, H. (2011). Genetic and epigenetic networks in intellectual disabilities. Annu. Rev. Genet. *45*, 81–104.

van Gaalen, M.M., and Steckler, T. (2000). Behavioural analysis of four mouse strains in an anxiety test battery. Behav. Brain Res. *115*, 95–106.

Vashishtha, M., Ng, C.W., Yildirim, F., Gipson, T.A., Kratter, I.H., Bodai, L., Song, W., Lau, A., Labadorf, A., Vogel-Ciernia, A., et al. (2013). Targeting H3K4 trimethylation in Huntington disease. Proc. Natl. Acad. Sci. USA *110*, E3027–E3036.

Xu, J., Deng, X., and Disteche, C.M. (2008). Sex-specific expression of the X-linked histone demethylase gene Jarid1c in brain. PLoS ONE *3*, e2553.